Visualizing probability distributions across bivariate cyclic temporal granularities

Sayani Gupta *

Department of Econometrics and Business Statistics, Monash University

and

Rob J Hyndman

Department of Econometrics and Business Statistics, Monash University

and

Dianne Cook

Department of Econometrics and Business Statistics, Monash University

and

Antony Unwin

University of Augsburg

July 30, 2020

Abstract

Deconstructing a time index into time granularities can assist in exploration and automated analysis of large temporal data sets. This paper describes several classes of time deconstructions using linear and cyclic time granularities. Linear time granularities respect the linear progression of time such as hours, days, weeks and months with respect to a baseline. Cyclic time granularities can be circular such as hour of the day, quasi-circular such as day of the month, and aperiodic such as public holidays. The hierarchical structure of granularities creates a nested ordering. Hour of the day and second of the minute are single-order-up. Hour of the week is multiple-order-up, because it passes over day of the week. Methods are provided for creating all possible granularities for a time index. A recommendation algorithm provides an indication whether a pair of granularities can be meaningfully examined together, called a harmony or when they cannot, called a clash.

The time granularities can be used to create visualizations of the data to explore for periodicities, associations and anomalies. The granularities can be considered to be categorical variables (ordered or unordered) which induces a grouping of the observations. Assuming a numeric response variable, the resulting graphics are then

---

*Email: Sayani.Gupta@monash.edu

displays of distributions compared across combinations of categorical variables. A recommendation of appropriate distribution display is provided.

The methods are implemented in the open source R package `gravitas`. The functions for creating granularities and exploring the associated time series are consistent with a tidy workflow (Grolemund & Wickham (2017)), and the probability distributions can be examined using the range of graphics available in `ggplot2` (Wickham 2016).

1 Introduction

Temporal data are available at various resolutions depending on the context. Social and economic data like GDP is often collected and reported at coarse temporal scales such as monthly, quarterly or annually. With recent advancement in technology, more and more data are recorded at much finer temporal scales. Energy consumption may be collected every half an hour, energy supply may be collected every minute, and web search data might be recorded every second. As the frequency of data increases, the number of questions about the periodicity of the observed variable also increases. For example, data collected at an hourly scale can be analyzed using coarser temporal scales such as days, months or quarters. This approach requires deconstructing time in various possible ways called time granularities (Aigner et al. 2011).

It is important to be able to navigate through all of these time granularities to have multiple perspectives on the periodicity of the observed data. This idea aligns with the notion of EDA (Tukey 1977) which emphasizes the use of multiple perspectives on data to help formulate hypotheses before proceeding to hypothesis testing. Visualizing probability distributions conditional on one or more granularities is an indispensable tool for exploration. Analysts are expected to comprehensively explore the many ways to view and consider temporal data. However, the plethora of choices and the lack of a systematic approach to do so quickly becomes overwhelming.

Calendar-based graphics (Wang et al. 2020a) are useful in visualizing patterns in the weekly and monthly structure, and are helpful when checking for the effects of weekends or special days. Any temporal data at sub-daily resolution can also be displayed using this type of faceting (Wickham 2016) with days of the week, month of the year, or another sub-daily deconstruction of time. But calendar effects are not restricted to conventional day-of-week or month-of-year deconstructions. There can be many different time deconstructions, based on the calendar or on categorizations of time granularities.

Linear time granularities respect the linear progression of time and are non-repeating such as hours, days, weeks and months. One of the first attempts to characterize these granularities is due to Bettini et al. (1998). However, the definitions and rules defined are inadequate for describing cyclic or repeating granularities. Hence, there is a need to

define some new cyclic time granularities, that can be useful in visualizations. Cyclic time granularities can be circular, quasi-circular or aperiodic. Examples of circular granularities are hour of the day and day of the week; an example of a quasi-circular granularity is day of the month; examples of aperiodic granularities are public holidays and school holidays.

Time deconstructions can also be based on the hierarchical structure of time. For example, hours are nested within days, days within weeks, weeks within months, and so on. Hence, it is possible to construct single-order-up granularities such as second of the minute, or multiple-order-up granularities such as second of the hour. The lubridate package (Grolemund & Wickham 2011) provides tools to access and manipulate common date-time objects. However, most of its accessor functions are limited to single-order-up granularities.

The motivation for this work stems from the desire to provide methods to better understand large quantities of measurements on energy usage reported by smart meters in households across Australia, and indeed many parts of the world. Smart meters currently provide half-hourly use in kWh for each household, from the time that they were installed, some as early as 2012. Households are distributed geographically and have different demographic properties such as the existence of solar panels, central heating or air conditioning. The behavioral patterns in households vary substantially, for example, some families use a dryer for their clothes while others hang them on a line, and some households might consist of night owls, while others are morning larks. It is common to see aggregates (see Goodwin & Dykes 2012) of usage across households, such as half-hourly total usage by state, because energy companies need to plan for maximum loads on the network. But studying overall energy use hides the distribution of usage at finer scales, and makes it more difficult to find solutions to improve energy efficiency. We propose that the analysis of smart meter data will benefit from systematically exploring energy consumption by visualizing the probability distributions across different deconstructions of time to find regular patterns/anomalies. Although, the motivation came through the smart meter example, this is a problem that is relevant to any temporal data observed more than once per year.

This work provides tools for systematically exploring bivariate granularities within the tidy workflow. In particular, we

4

- provide a formal characterization of cyclic granularities;

- facilitate manipulation of single- and multiple-order-up time granularities through cyclic calendar algebra;

- develop an approach to check the feasibility of creating plots or drawing inferences for any two cyclic granularities;

- recommend prospective probability distributions for exploring distributions of a univariate dependent variable across pair of granularities.

The remainder of the paper is organized as follows: Section 2 provides some background material on linear granularities and calendar algebra for computing different linear granularities. Section 3 formally characterizes different cyclic time granularities by extending the framework of linear time granularities. Section 3.4 introduces cyclic calendar algebra for computing cyclic time granularities. Section 4 discusses the data structure for exploring the conditional distributions of the associated time series across pairs of cyclic time granularities. Section 5 discusses the role of different factors in constructing an informative and trustworthy visualization. Section 6 examines how systematic exploration can be carried out for a temporal and non-temporal application. Section 7 summarizes this paper and discusses possible future direction.

2 Linear time granularities

Discrete abstraction of time such as weeks, months or holidays can be thought of as "time granularities". Time granularities are **linear** if they respect the linear progression of time. There have been several attempts to provide a framework for formally characterizing time granularities, including Bettini et al. (1998) which forms the basis of the work described here.

2.1 Definitions

Definition 1. *A **time domain** is a pair $(T; \leq)$ where T is a non-empty set of time instants and $\leq$ is a total order on T.*

hour	0	1	...	23	24	25	...	47	...	144	...	167	...	...	...	720	...	743	...	...	...	...	...	...	...	...	...	...	...	...	t
day	0				1				...	6			...			31			...					365		...			...		t/24
week	0										...		5				....		53			...			....			t/24*7
month	0														...		12			...	...			M
year	0															...			Y

Figure 1: Illustration of time domain, linear granularities and index set. Hour, day, week, month and year are linear granularities and can also be considered to be time domains. These are ordered with ordering guided by integers and hence is unidirectional and non-repeating. Hours could also be considered the index set, and a bottom granularity.

The time domain is assumed to be *discrete*, and there is unique predecessor and successor for every element in the time domain except for the first and last.

Definition 2. *There is a unique* **index set**, $Z = \{z : z \in \mathbb{Z}_{\geq 0}\}$, *which map the time instants to a set of non-negative integers. Often, this is thought of as $t = 0, \ldots, T$.*

Definition 3. *A* **linear granularity** *is a mapping G from the integers (the index set, Z) to subsets of the time domain such that: (1) if $i < j$ and $G(i)$ and $G(j)$ are non-empty, then each element of $G(i)$ is less than all elements of $G(j)$; and (2) if $i < k < j$ and $G(i)$ and $G(j)$ are non-empty, then $G(k)$ is non-empty. Each non-empty subset $G(i)$ is called a* **granule**.

This implies that the granules in a linear granularity are non-overlapping, continuous and ordering is maintained. The indexing for each granule can also be associated with textual representation, called the label. A discrete time model often uses a fixed smallest linear granularity named by Bettini et al. (1998) **bottom granularity**. Figure 1 illustrates the linear time granularities. Here, "hour" is the bottom granularity and "day", "week", "month" and "year" are linear granularities which maps from index set to subsets of the hourly time domain. If we have "hour" running from $\{0, 1, \ldots, t\}$, we will have "day" running from $\{0, 1, \ldots, \lfloor t/24 \rfloor\}$. These linear granularities are ordered with ordering guided by the index set which is a set of integers. Hence, they are uni-directional and non-repeating.

2.2 Relativities

Properties of pairs of granularities fall into various categories.

Definition 4. *A linear granularity G is* **finer than** *a linear granularity H, denoted $G \preceq H$, if for each index i, there exists an index j such that $G(i) \subset H(j)$.*

Definition 5. *A linear granularity G* **groups into** *a linear granularity H, denoted $G \unlhd H$, if for each index j there exists a (possibly infinite) subset S of the integers such that $H(j) = \bigcup_{i \in S} G(i)$.*

Example. Both *day $\unlhd$ week* and *day $\preceq$ week* holds, since every granule of *week* is the union of some set of granules of day and each day is a subset of a *week*. Consider another example where *day $\unlhd$ month*. This relationship however is incomplete without its association to periodicity. Each month is a grouping of the same number of days over years, hence the period of the grouping $(day, month)$ is one year, if leap years are ignored. This grouping period becomes 4 and 400 years with the inclusion of leap years and leap seconds respectively.

Definition 6. *A granularity G is* **periodical** *with respect to a granularity H if: (1) $G \unlhd H$; and (2) there exist $R, P \in \mathbb{Z}_+$, where R is less than the number of granules of H, such that for all $i \in \mathbb{Z}$, if $H(i) = \bigcup_{j \in S} G(j)$ and $H(i + R) \neq \phi$ then $H(i + R) = \bigcup_{j \in S} G(j + P)$.*

If $S_0, \ldots, S_{R-1}$ are the sets of indexes of G describing $H(0), \ldots, H(R-1)$, respectively, then the description of an arbitrary granule $H(j)$ is given by $\bigcup_{i \in S_{j \mod R}} G(P * \lfloor j/R \rfloor + i)$. Also, granularities can be periodical with respect to other granularities, except for a finite number of spans of time where they behave in an anomalous way, called **quasi-periodic** relationships by Bettini & De Sibi (2000).

Example. In a Gregorian calendar without leap years we could say *day* groups periodically into month with the period $P = 365$ and the number of granules of *month* in each period given by $R = 12$. In a Gregorian calendar with leap years, *day* groups quasi-periodically into *month* with the exceptions of the time domain corresponding to 29th February of any year.

Definition 7. *The **order** of a linear granularity is the level of coarseness associated with a linear granularity. A linear granularity G will have lower order than H if each granule of G is composed of lower number of granules of bottom granularity than each granule of H.*

Example. For two linear granularities G and H, if G *groups into* or *finer than H* then G is of lower order than H. Moreover, if we consider bottom granularity as day, linear granularity week will have lower order than month since each week consist of less number of days than each month. Here neither week *groups into* month or week *finer than* month, but their relative order could be determined.

2.3   Computation

Granules in bottom granularity or any finer granularity may be aggregated in some manner to form larger granules belonging to a coarser granularity. A system of multiple granularities in lattice structures is referred to as a **calendar** by Dyreson et al. (2000). Linear time granularities are computed through an algebraic representation for time granularities, which is referred to as calendar algebra (Ning et al. 2002). It is assumed that there exists a *bottom granularity* and calendar algebra operations are designed to generate new granularities recursively from the bottom one. Some relevant calendar algebra operations are discussed below; these will be used in Section 3 for illustrations in circular and quasi-circular granularities.

Definition 8. *Let G_1 be a full-integer labelled granularity, and m a positive integer. **The grouping operation** $Group_m(G)$ generates a new granularity G_2, by partitioning the granules of G_1 into m-granule groups and making each group a granule of the resulting granularity. More precisely, $G_2 = Group_m(G_1)$ is the full-integer labelled granularity such that for each integer i,*

$$G_2(i) = \bigcup_{j=(i-1)m+1}^{im} G_1(j).$$

The grouping operation $Group_m(G)$, provides a new granularity whose granules are the integer part of the quotient when the integer set spanned by linear granularity G is divided by m, such that, $G_2(i) = \lfloor G_1(j)/m \rfloor$.

Example. Due to even length of *day* and *week*, we can derive them from *hour* using the grouping operation as follows: day = G_{24}(hour), week = G_{24*7}(hour).

For more variations of calendar algebra operations, see Ning et al. (2002).

3   Cyclic time granularities

Cyclic granularities represent cyclical repetitions in time. They can be thought of as additional categorizations of time that are not linear. Cyclic granularities can be constructed by operating on two linear granularities. Cycles can be either *regular*, called **circular**, or *irregular*, **quasi-circular** when these two linear granularities relate periodically.

3.1   Circular

Definition 9. *A* **circular granularity** $C_{B,G}$ *relates a linear granularity G to the bottom granularity B, if*

$$C_{B,G}(z) = z \ mod \ P(B,G) \quad \forall z \in \mathbb{Z}_{\geq 0} \tag{1}$$

where z denotes the index set, B denotes a full-integer labelled bottom granularity which groups periodically into linear granularity G with regular mapping, and $P \equiv P(B,G)$ is the number of granules of B in each granule of G, also called the period of the grouping (B,G).

Example. Figure 2 illustrates the linear and the corresponding cyclical granularities. Cyclical granularities can be considered to be cutting the linear granularity into pieces, and stacking them to match the cycles (as shown in b). B, G, H (day, week, fortnight, respectively) are linear granularities. The circular granularity $C_{B,G}$ (day-of-week)is constructed from B and G. The circular granularity $C_{B,H}$ (day-of-fortnight) is constructed from B and H. These overlapping cyclical granularities share elements from the linear granularity. Each of $C_{B,G}$ and $C_{B,H}$ consist of repeated patterns $\{0, 1, 2, \ldots, 6\}$ and $\{0, 1, 2, \ldots, 13\}$ with $P = 7$ and $P = 14$ respectively. Each circular granularity can use descriptive label mappings. Suppose L is a label mapping that defines an unique label for each index $l \in \{0, 1, \ldots, (P-1)\}$, then the label mapping L for $C_{B,G}$ can be defined as

$$L : \{0, 1, 2, \ldots, 6\} \longmapsto \{\text{Sun}, \text{Mon}, \ldots, \text{Sat}\}$$

a

days (B)	0	1	2	3	4	5	6	7	8	9	10	11	12	13	14	15	16	17	18	19	20	21	22	23	24	25	26	27
weeks (G)	0							1							2							3						
fortnights (H)	0														1													
$C_{B,G}$	0	1	2	3	4	5	6	0	1	2	3	4	5	6	0	1	2	3	4	5	6	0	1	2	3	4	5	6
$C_{B,H}$	0	1	2	3	4	5	6	7	8	9	10	11	12	13	0	1	2	3	4	5	6	7	8	9	10	11	12	13

b

weeks

0	1	2	3	4	5	6
0	1	2	3	4	5	6
0	1	2	3	4	5	6
0	1	2	3	4	5	6

...

fortnights

0	1	2	3	4	5	6	7	8	9	10	11	12	13
0	1	2	3	4	5	6	7	8	9	10	11	12	13
0	1	2	3	4	5	6	7	8	9	10	11	12	13
0	1	2	3	4	5	6	7	8	9	10	11	12	13

...

Figure 2: Illustration of circular relative to linear granularities (a). Circular granularities can be considered to be cutting the linear granularity into pieces and stacking them (b). The circular granularity creates repeated integer sequences.

or

$$L : \{0, 1, 2, \ldots, 6\} \longmapsto \{\text{Sunday}, \text{Monday}, \ldots, \text{Saturday}\}$$

for example.

In general, any circular granularity relating two linear granularity can be expressed as $C_{(G,H)}(z) = \lfloor z/P(B,G) \rfloor \bmod P(G,H)$, where linear granularity H is periodic with respect to linear granularity G with regular mapping and $P(G,H)$ is the period of the grouping (G,H). Table 1 shows representation of circular granularities C_i relating two linear granularities with period P_i and minutes as the bottom granularity.

3.2 Quasi-circular

A **quasi-circular** granularity can not be defined using modular arithmetic since they are formed using two linear granularities with irregular mapping. However, they are still formed with linear granularities, one of which "groups periodically into" the other. Table 2 shows

circular granularity	expression	period
minute-of-hour	$C_1 = z \bmod 60$	$P_1 = 60$
minute-of-day	$C_j = z \bmod 60 * 24$	$P_2 = 1440$
hour-of-day	$C_3 = \lfloor z/60 \rfloor \bmod 24$	$P_3 = 24$
hour-of-week	$C_4 = \lfloor z/60 \rfloor \bmod 24 * 7$	$P_4 = 168$
day-of-week	$C_5 = \lfloor z/24 * 60 \rfloor \bmod 7$	$P_5 = 7$

Table 1: Examples of circular granularities with bottom granularity minutes. Circular granularity C_i relates two linear granularities one of which groups periodically into the other with regular mapping and period P_i. Circular granularities can be expressed using modular arithmetic due to their regular mapping.

some example of quasi-circular granularities (Q_i) with (P_i) denoting the plausible choices of period of the grouping of two linear granularities.

quasi-circular granularity	potential period lengths
$Q_1 = $ day-of-month	$P_1 = 31, 30, 29, 28$
$Q_2 = $ hour-of-month	$P_2 = 24 * 31, 24 * 30, 24 * 29, 24 * 28$
$Q_3 = $ day-of-year	$P_3 = 366, 365$
$Q_4 = $ week-of-month	$P_4 = 5, 4$

Table 2: Examples of quasi-circular granularities Q_i with potential period lengths P_i. These quasi-circular granularities relate two linear granularities one of which groups periodically into the other with irregular mapping leading to many potential period lengths and hence can not be expressed through modular arithmetic.

Definition 10. *A* **quasi-circular granularity** $Q_{B,G'}$ *relates linear granularities G' and bottom granularity B, if*

$$Q_{B,G'}(z) = z - \sum_{w=0}^{k-1} |T_{w \bmod R'}|, \quad for \quad z \in T_k \tag{2}$$

where, $z \in \mathbb{Z}_{\geq 0}$ denotes the index set, B denotes a full-integer labelled bottom granularity which groups periodically into linear granularity G' with irregular mapping, P' and R' are

the period of the grouping (B, G') and the number of granules of G' in P', T_w are the sets of indices of B describing $G'(w)$ such that $G'(w) = \bigcup_{z \in T_w} B(z)$ and $|T_w|$ is the cardinality of set T_w.

Example. Consider G' such that every two consecutive granules of G' are made up of 7 and 5 granules of B respectively within each period of the grouping (B, G'). Then $Q_{B,G'}$ is a repetitive categorization of time, similar to circular granularities, except that the number of granules of B is not necessarily the same across different granules of G'. Here, $T_0 = \{0, 1, 2, 3, 4, 5, 6\}$ and $T_1 = \{7, 8, 9, 10, 11\}$. Hence using Definition 10 we will have:

$$Q_{B,H'}(10) = 10 - \sum_{w=0}^{1-1} |T_{w \bmod 2}|, \quad since \quad 10 \in T_1$$

$$= 3$$

If linear granularity G' is periodical with respect to B with irregular mapping, then there exist $R', P' \in \mathbb{Z}_+$ such that if $G'(w) = \bigcup_{z \in T_w} B(z)$ then

$$G'(w) = \bigcup_{z \in T_{w \bmod R'}} B(P' * \lfloor w/R' \rfloor + z)$$

(from Definition 6) . Here $w \bmod R'$ represents the index that must be shifted to obtain $G'(w)$. The idea here is if we know the composition of each of the granules of G' in terms of granules of B for one period, we can find the composition of any granule of G' beyond a period since the "pattern" repeats itself along the time domain due to the periodic property. The periodic property also ensures that $|T_w| = |T_{w \bmod R'}|$ since every wth and $(w + R')^{\text{th}}$ granule of G' will have the same number of granules of B. The term $\sum_{w=0}^{k-1} |T_w|$ in Definition 10 denotes the number of granules of B till the $(k-1)^{\text{th}}$ granule of G'. Since $|T_w| = |T_{w \bmod R'}|$, the number of granules of B till the $(k-1)^{\text{th}}$ granule of G' becomes $\sum_{w=0}^{k-1} |T_{w \bmod R'}|$ in Definition 10.

3.3 Aperiodic

Aperiodic time granularities are the ones which can not be specified as a periodic repetition of a pattern of granules. Most public holidays repeat every year, but there is no reasonably

small period within which their behavior remains constant. A classic example can be that of Easter, whose dates repeat only after 5,700,000 years. In Australia, if a standard public holiday falls on a weekend, a substitute public holiday will sometimes be observed on the first non-weekend day (usually Monday) after the weekend. Examples of aperiodic granularity may also include school holidays or a scheduled event. All of these are recurring events, but with non-periodic patterns. As such, plausible P_i from Table 2 could be possibly infinite for aperiodic granularities.

Aperiodic cyclic granularities are defined using aperiodic linear granularities. Consider n aperiodic linear granularities $M_i \forall \{i \in 1, 2, \ldots, n\}$ such that Definition 6 does not hold true for them with respect to B (the bottom granularity). However, $B \trianglelefteq M_i \forall \{i \in 1, 2, \ldots, n\}$. Then according to Definition 5, for each index j there exists a (possibly infinite) subset $T_{\{i_j\}}$ of the integers such that $M_i(j) = \bigcup_{z \in T_{i_j}} B(z)$. Suppose $M = \bigcup_{i=1}^{n} M_i$ is formed by collecting the granules of $\{M_1, M_2, \ldots, M_n\}$. Here, index $\{i_j\}$ stands for the jth granule of the ith linear aperiodic granularity.

Definition 11. *An **aperiodic cyclic granularity** $A_{B,M}$ relates a linear granularity M to the bottom granularity B, if*

$$A_{B,M}(z) = \begin{cases} i, & for \quad z \in T_{i_j} \\ 0 & otherwise \end{cases} \tag{3}$$

where, $z \in \mathbb{Z}_{\geq 0}$ denotes the index set, B denotes a full-integer labelled bottom granularity which groups into linear granularity M but not periodically, T_{i_j} are the sets of indices of B describing aperiodic linear granularities M_i such that $M_i(j) = \bigcup_{z \in T_{i_j}} B(z)$, and $M = \bigcup_{i=1}^{n} M_i$.

Example. Consider a school semester which always lasts for 18 weeks and 2 days, starting with one week of orientation followed by an in-session period of 6 weeks, a semester-break of 1 week and again an in-session period of 7 weeks and 1 week study break before final exams which continue for 16 days. Let the linear granularities M_1 and M_2 denote in-session semester period and semester break periods respectively. Both M_1, M_2 and $M = M_1 \bigcup M_2$ denoting the semester week type are aperiodic with respect to days (B) or weeks (G). Hence $A_{B,M}$ denoting day of the semester week type would be an aperiodic cyclic granularity. This

a

days (B)	0	1	...	48	49 ... 55	56 ... 62	...	91 ... 97	98 ... 104	105 ... 111	...	147 ... 153	154 ... 160	161 ... 167	168 ... 174	175	176	. ... .
weeks (G)	0	0	...	6	7	8	...	13	14	15	...	21	22	23	24	25		
sem wk (H)	-	-	...	-	0	1	...	6	7	8	...	14	15	16	17	18	-	-
sem wk type (M)	-	-	...	-	0		1		2	3			4	5			-	-
$Q_{H,M}$	-	-	...	-	0	0	...	5	0	0	...	6	0	0	1	2	-	-
$A_{B,M}$	0	0	...	0	1 1 1	2 2 2	...	2 2 2	1 1 1	2 2 2	...	2 2 2	1 1 1	2 2 2	2 2 2	2	2	0 ... 0

b

semester weeks

- 0 — "orientation week"
- 0 | 1 | 2 | 3 | 4 | 5 — "first half of semester"
- 0 — "semester break"
- 0 | 1 | 2 | 3 | 4 | 5 | 6 — "second half of semester"
- 0 — "study week"
- 0 | 1 | 2 — "finals"

Figure 3: Quasi-circular and aperiodic cyclic granularities illustrated through linear (a) and stack (b) display of time. The linear display shows linear granularities days, weeks, semester weeks, semester week type distributed linearly from past to future. Here a semester lasts for 18.3 weeks, each starting with one week of orientation followed by an in-session period of 6 weeks, a semester-break of 1 week and again an in-session period of 7 weeks and 1 week study break before final exams which continue for 1.3 weeks. This pattern remains same for all semester and hence $Q_{H,M}$ with $P = 18.3$ weeks will be a quasi-circular granularity with repeating patterns. $A_{B,M}$ will be an aperiodic cyclic granularity since the placement of the semester within an year varies across years.

is because the placement of the semester within an year would vary across years. Figure 3 b shows the stack display of time with granules representing same categories (semester break/in-session) stacked on top of one another. Figure 3 (a) representing the linear display of time is useful in manifesting how the categories would be determined with respect to the bottom granularities using Definition 11. It is interesting to note here that $Q_{H,M}$ denoting semester week of the semester week type would be a quasi-circular granularity since the distribution of semester weeks within a semester is assumed to remain constant over years. Here $Q_{H,M}$ with a period of 18.3 weeks will have irregular mapping since each semester week types consists of different number of semester weeks.

3.4   Relativities

The hierarchical structure of time creates a natural nested ordering which can be used in the computation of relative pairs of granularities. This is illustrated using two examples, a Mayan calendar, which is simple, in addition to the more complex Gregorian calendar.

Definition 12. *The nested ordering of linear granularities can be organized into a* **hierarchy table***, denoted as $H_n : (G, C, K)$, which arranges them from lowest to highest in order. It shows how the n granularities relate through K, and how the cyclic granularities, C. can be defined relative to the linear granularities. Let G_l and G_m represent the linear granularity of order l and m respectively with $l < m$. Then $K \equiv P(l, m)$ represents the period length of the grouping (G_l, G_m), if C_{G_l, G_m} is a circular granularity and $K \equiv k(l, m)$ represents the operation to obtain G_m from G_l, if C_{G_l, G_m} is quasi-circular.*

Example. Table 3 shows the hierarchy table for the Mayan calendar. In the Mayan calendar, one day is referred to as a kin and the calendar was structured such that 1 kin = 1 day; 1 uinal = 20 kin; 1 tun = 18 uinal (about a year); 1 katun = 20 tun (20 years) and 1 baktun = 20 katun.

It is interesting to note, that in the Mayan calendar, like most calendars, that day is the basic unit of time (Reingold & Dershowitz 2001). The structuring of larger units, weeks, months, years and cycle of years, though, varies substantially. An exception is the French revolutionary calendar, which divides each day into 10 "hours", each "hour" into 100

Table 3: Hierarchy table for Mayan calendar with circular single-order-up granularities.

linear (G)	single-order-up cyclic (C)	period length/conversion operator (K)
kin	kin-of-uinal	20
uinal	uinal-of-tun	18
tun	tun-of-katun	20
katun	katun-of-baktun	20
baktun	1	1

"minutes" and each "minute" into 100 "seconds", the duration of which is 0.864 common seconds. Nevertheless, for any calendar a hierarchy table can be defined.

Note that, it is not always possible to organize an aperiodic linear granularity in a hierarchy table. Hence, we assume that the hierarchy table consists of periodic linear granularities only and that the cyclic granularity $C_{G(l),G(m)}$ is either circular or quasi-circular.

Definition 13. *The hierarchy table contains* **multiple-order-up** *granularities which are cyclic granularities that are nested within multiple levels. A* **single-order-up** *is a cyclic granularity which is nested within a single level. It is a special case of multiple-order-up granularity.*

Example. In Table 3, kin-of-tun or kin-of-baktun are examples of multiple-order-up granularities and single-order-up granularities are kin-of-uinal, uinal-of-tun etc.

3.5 Computation

In this section, we will see how to obtain cyclic granularities through an algebraic representation of other cyclic granularities. This is similar to calendar algebra in **?** for linear granularities but caters to computation of cyclic granularities, we shall refer to it as through cyclic calendar algebra operations. The cyclic calendar algebra consists of broadly two kinds of operations: (1) **single-to-multiple** and (2) **multiple-to-single** which entails the representation of *multiple-order-up* cyclic granularities from *single-order-up* cyclic granularities

respectively.

3.5.1 Single-to-multiple

Methods to obtain multiple-order-up granularity will be different based on if the hierarchy consists of all circular single-order-up granularities or a mix of circular and quasi-circular single-order-up granularities. The methods require the use of integer arithmetic, and hence it is important that the label mapping of the individual single-order-up granularity is an identity function, that is, $L(x) = x \quad \forall x$. The label mapping of the resultant multiple-order-up granularity can be chosen depending on the context. Circular single-order-up granularities can be used recursively to obtain a multiple-order-up circular granularity using Equation 4 for $l < m - 1$ and $P(i, j) = 1, \quad \forall i = j \in \{0, 1, \ldots, m - l - 1\}$.

$$
\begin{aligned}
C_{G_l,G_m}(z) &= C_{G_l,G_{l+1}}(z) + P(l, l+1)C_{G_{l+1},G_m}(z) \\
&= C_{G_l,G_{l+1}}(z) + P(l, l+1)(C_{G_{l+1},G_{l+2}}(z) + P(l+1, l+2)C_{G_{l+2},G_m}(z)) \\
&= C_{G_l,G_{l+1}}(z) + P(l, l+1)C_{G_{l+1},G_{l+2}}(z) + P(l, l+1)P(l+1, l+2)C_{G_{l+2},G_m} \\
&= C_{G_l,G_{l+1}}(z) + P(l, l+1)C_{G_{l+1},G_{l+2}}(z) + P(l, l+2)C_{G_{l+2},G_{l+m}}(z) \quad (4) \\
&\vdots \\
&= \sum_{i=0}^{m-l-1} P(l, l+i)C_{G_{l+i},G_{l+i+1}}(z)
\end{aligned}
$$

For example, the multiple-order-up granularity $C_{uinal,katun}$ for Mayan calendar could be obtained using Equation 5.

$$
\begin{aligned}
C_{uinal,baktun}(z) =& C_{uinal,tun}(z) + P(uinal, tun)C_{tun,katun}(z) + P(uinal, katun)C_{katun,baktun}(z) \\
=& \lfloor z/20 \rfloor \bmod 18 + 18 * \lfloor z/20 * 18 \rfloor \bmod 20 \\
& + 18 * 20 \lfloor z/20 * 18 * 20 \rfloor \bmod 20
\end{aligned}
$$

$$(5)$$

We consider the case of only one quasi-circular single order-up granularity in the hierarchy table while computing a multiple-order-up quasi-circular granularity. Any multiple-order-up quasi-circular granularity $C_{l,m}(z)$ could then be obtained as a dicrete combination of

Table 4: Hierarchy table for the Gregorian calendar with both circular and quasi-circular single-order-up granularities.

linear (G)	single-order-up cyclic (C)	period length/conversion operator (K)
minute	minute-of-hour	60
hour	hour-of-day	24
day	day-of-month	k(day, month)
month	month-of-year	12
year	1	1

circular and quasi-circular granularities. Depending on the order of the combination, again two different approaches need to be employed leading to the following cases:

- $C_{l,m'}(z)$ is circular and $C_{m',m}(z)$ is quasi-circular

$$C_{G_l,G_m}(z) = C_{G_l,G_{m'}}(z) + P(l,m')C_{G_{m'},G_m}(z) \tag{6}$$

- $C_{l,m'}(z)$ is quasi-circular and $C_{m',m}(z)$ is circular

$$C_{G_l,G_m}(z) = C_{G_l,G_{m'}}(z) + \sum_{w=0}^{C_{m',m}(z)-1} (|T_w|) \tag{7}$$

where, T_w is such that $G_{m'}(w) = \bigcup_{z \in T_w} G_l$ and $|T_w|$ is the cardinality of set T_w.
Consider a hierarchy using linear granularties from a Gregorian calendar in Table 4. This is an example of a hierarchy structure which has both circular and quasi-circular single-order-up granularities with day-of-month as the only single-order-up quasi-circular granularity. Using Equations 6 and 7, we then have:

$$C_{hour,month}(z) = C_{hour,day}(z) + P(hour, day) * C_{day,month}(z)$$

$$C_{day,year}(z) = C_{day,month}(z) + \sum_{w=0}^{C_{month,year}(z)-1} (|T_w|)$$

, where T_w is such that $month(w) = \bigcup_{z \in T_w} day(z)$

18

3.5.2 Multiple-to-single

Similar to single-to-multiple operations, multiple-to-single operations also involve different approaches for all circular single-order-up granularities and a mix of circular and quasi-circular single-order-up granularities in the hierarchy. For a hierarchy table $H_n : (G, C, K)$ with only circular single-order-up granularities in the hierarchy and $l_1, l_2, m_1, m_2 \in 1, 2, \ldots, n$ and $l_2 < l_1$ and $m_2 > m_1$, multiple-order-up granularities could be obtained using 8.

$$C_{G_{l_1}, G_{m_1}}(z) = \lfloor C_{G_{l_2}, G_{m_2}}(z) / P(l_2, l_1) \rfloor \bmod P(l_1, m_1) \tag{8}$$

For example, in Mayan Calendar, it is possible to compute the single-order-up granularity tun-of-katun from uinal-of-baktun, since $C_{tun, katun}(z) = \lfloor C_{uinal, baktun}(z) / 18 \rfloor \bmod 20$.

Multiple order-up quasi-circular granularities   Single-order-up quasi-circular granularity could be obtained from multiple-order-up quasi-circular granularity and single/multiple-order-up circular granularity using Equations 6 and 7.

4   Data structure

Effective exploration and visualization benefits from well-organized data structures. Wang et al. (2020b) introduced a tidy data structure, tsibble, to support exploration and modeling of temporal data. This forms the basis of the structure for cyclic granularities. A tsibble consists of an index, key and measured variables. An index is a variable with inherent ordering from past to present and a key is a set of variables that define observational units over time. A linear granularity is a mapping of the index set to subsets of the time domain. For example, if the index of a tsibble is days, then a linear granularity might be weeks, months or years. A bottom granularity is represented by the index of the tsibble.

All cyclic granularities can be expressed in terms of the index set, and hence, we introduce the data structure in Figure 4. This basic structure of a tsibble (index, key, measurements) is augmented by columns of cyclic granularities.The total number of cyclic granularities would be based on the number of linear granularities considered in the hierarchy table and presence of any aperiodic cyclic granularities, for example, if we have n periodic linear

granularities in the hierarchy table, $n(n-1)/2$ circular or quasi-circular cyclic granularities could be constructed. Let N_C be the total number of contextual circular, quasi-circular and aperiodic cyclic granularities that could originate from N_L periodic and aperiodic linear granularities. Any attempt to encode all or many of these cyclic granularities at the same time to develop insights on periodicity might fail or otherwise become too numerous for comprehensive human consumption. Instead, this big problem is broken down by focusing on pair of cyclic granularities (C_i, C_j) at a time for $i, j \in \{1, 2, \ldots, N_C\}$. Data sets of the form $<C_i, C_j, v>$ then forms the basis for exploration and analysis of the measured variable v.

index	key	measurements	C_1	C_2	....	C_i	...	C_j	...	C_{Nc}

Figure 4: The data structure for exploring periodicities in data by including cyclic granularities in the tsibble structure with index, key and measured variables.

4.1 Harmonies and clashes

The way cyclic granularities relate become important when we consider the data structure in Figure 4. Let us consider two cyclic granularities C_i and C_j, such that C_i maps index set to a set $\{A_k | k \in \mathbb{N}, k \leq K\}$ and C_j maps index set to a set $\{B_l | l \in \mathbb{N}, l \leq L\}$. Here, A_k's or B_l's are the levels/categories corresponding to C_i and C_j respectively. Let S_{kl} be a subset of the index set such that for all $s \in S_{kl}$, $C_i(s) = A_k$ and $C_j(s) = B_l$. Data subsets for each combination of levels (A_k, B_l) like $<A_k, B_l, v(s)>$ can be obtained for all $k \in 1, 2, \ldots, K$ and $l \in 1, 2, \ldots, L$ which will lead to KL data subsets. Now, some situations can lead to few or many of these sets being empty. We will discuss few cases, where one or more of these KL sets will be empty either due to the structure of the calendar, duration and location of events in a calendar or just by the construction of the cyclic granularities.

Definition 14. *A **clash** is a pair of cyclic granularities which contains structurally, event-driven or build-based empty combinations of its categories.*

Definition 15. *A **harmony** is a pair of cyclic granularities that does not contain any empty combinations of its categories.*

Firstly, empty combinations can arise due to the structure of the calendar or hierarchy. These are called "structurally" empty combinations. Let us take a specific example, where C_i be day-of-month with 31 levels and C_j be week-of-month with 5 levels. There will be $31 \times 5 = 155$ sets S_{kl} corresponding to possible combinations of C_i and C_j. Many of these like $S_{1,5}$, $S_{21,2}$ are empty. This is also intuitive since the first day of the month can never correspond to fifth week of the month. Hence the pair (day-of-month, week-of-month) is a clash.

Secondly, empty combinations can turn up due to differences in event location or duration in a calendar. These are called "event-driven" empty combinations. Let us consider C_i be day-of-week with 7 levels and C_j be WorkingDay/NonWorkingDay with 2 levels. While potentially all of these 14 sets S_{kl} can be non-empty (it is possible to have a public holiday on any day-of-week), in practice many of these will probably have very few observations. For example, there are few (if any) public holidays on Wednesdays or Thursdays in any given year in Melbourne, Australia.

Thirdly, empty combinations can be a result of how granularities are constructed. These are called "build-based" empty combinations. Let C_i be Business-days, which are days from Monday to Friday except holidays and C_j be day-of-month. Then the days denoting weekends in a month would not correspond to any Business days. This is different from structurally empty combinations because structure of the calendar does not lead to these missing combinations, but the construction of the granularities does.

An example when there will be no empty combinations could be where C_i and C_j maps index set to day-of-week and month-of-year respectively. Here C_i can have 7 levels while C_j can have 12 levels. So there are $12 \times 7 = 84$ sets S_{kl}. All of these are non-empty because every day-of-week can occur in every month. Hence, the pair (day-of-week, month-of-year) is a harmony.

4.2 Summarizing the measured variable

Restructuring time from linear to cyclic time granularities leads to re-organisation of the data structure, where each level of a cyclic granularity corresponds to multiple values of the measured variable. It is common to see summarization of these multiple values through aggregation or an unique summary statistic like mean or median to have each level of cyclic granularity correspond to an unique value of the measured variable. However, this approach hides the distributions of the measured variable induced by the re-organised data structure. Summarizing the distribution of the measured variable through these multiple observations could be a potential way to explore and bring forward different features of the data.

However, we need to consider the effect of number of observations on the summarization even for harmonies. Consider a data set with $(T + 1)$ observations, and two cyclic granularities C_i and C_j with L and M categories respectively. Let $nobs$ be the number of observations for a combination of levels from (C_i, C_j). Now, $nobs$ might be equal for all combinations on an average so that $nobs = (T + 1)/(LM)$ as $T \to \infty$ or ideally take any value between $\{0, 1, 2, \ldots, T\}$. The statistical transformation used for summarizing the measured variable for a combination should be chosen in line with $nobs$. For example, it might be useful to compute deciles only when $nobs \geq 10$. Rarely occurring categories such as the 366th day of the year, or the 31st day of the month are more likely to suffer from this problem.

5 Visualization

The grammar of graphics introduced a framework to construct statistical graphics by relating data space to the graphic space (Wilkinson 1999). The layered grammar of graphics proposed by Wickham (2016), which is an alternate and modified parametrization of the grammar suggests that graphics are made up of distinct layers of grammatical elements. Drawing from the grammar of graphics, if $<C_i, C_j, v>$ serves as the basis of visualizing the distribution of the measured variable, the following layers can be specified:

- Data: $<C_i, C_j, v>$

- Aesthetic mapping (mapping of variables to elements of the plot): C_i mapped to x position and v to y position
- Statistical transformation (data summarization): any descriptive or smoothing statistics that summarizes distribution of v
- Geometric objects (physical representation of the data): any geometry displaying distribution, for example, boxplot, letter value, violin, ridge or highest density region plots
- Facet (split plots): C_j

5.1   Choice of statistical transformations and geometric objects

Choice of plots are dictated by the statistical transformations and geometric objects used for the visualization. The basic plot choice for our data structure is the one that can display distributions. We will discuss few conventional and recent ways to plot distributions using both Kernel density estimates and descriptive statistics. Descriptive statistics based displays include box plots (Tukey 1977) or different variations of it like notched box plots (Mcgill et al. 1978). More recent ways are the letter-value box plot (Hofmann et al. 2017) or quantile plots which display quantiles instead of quartiles in a traditional boxplot. Kernel density based plots for displaying a distribution include violin plots (Hintze & Nelson 1998), summary plot (Potter et al. 2010), ridge line plots, highest density regions (HDR) box (Hyndman 1996). Each type of density display has different parameters, that need to be estimated given the data. Each is equipped with some benefits and challenges which should be borne in mind while using them for exploration.

5.2   Facet and aesthetic variables

5.2.1   Levels

The levels of cyclic granularities has a role to play on the choice of plots since space and resolution might become a problem with too many levels. A potential approach could be to categorize the levels as very high/high/medium/low for each cyclic granularity and define some criteria based on usual cognitive power, display size available and the aesthetic

mappings. Default values for these categorizations could be chosen based on levels of common temporal granularities like days of the month, days of the fortnight or days of the week.

5.2.2 Synergy of cyclic granularities

For data sets of the form $(C_i, C_j, v) \forall i, j \in N_C$, if there are levels of C_i (or C_j) not spanned by levels of C_j (or C_i), empty sets are formed leading to potential ineffective graphs. The conjecture is that the synergy of these cyclic granularities are thus playing a role while deciding if the resulting plot would be a good candidate for exploratory analysis. Harmonies are pairs of granularities that do not contain empty combinations and thus aid exploratory data analysis. Plotting Clashes should be avoided since they contain empty combinations. For illustration, Figure 5 (a) shows the distribution of half-hourly electricity consumption through letter value plot across months of the year faceted by quarters of the year. This plot does not work because every quarter does not correspond to all months of the year, for example, the first quarter of the year would never correspond to the month December of an year.

5.2.3 Interchangeability of mappings

We will discuss the effect of the mapping of cyclic granularities in this section. When we consider data sets of the form $<C_i, C_j, v>$ with C_i mapped to x position and C_j to facets, then A_k's are placed in close proximity and each B_l represent a group/facet. Gestalt theory suggests that when items are placed in close proximity, people assume that they are in the same group because they are close to one another and apart from other groups. Hence, in this case A_k's are compared against each other within each group. With the mapping of C_i and C_j reversed, emphasis will shift to different behavior of the variables. Figure 5 (b) shows the letter value plot across weekday/weekend faceted by quarters of the year and Figure 5 (c) shows the same two cyclic granularities with their mapping reversed. Figure 5 (b) helps us to compare weekday and weekend within each quarter and Figure 5 (c) helps to compare quarters within weekend and weekday.
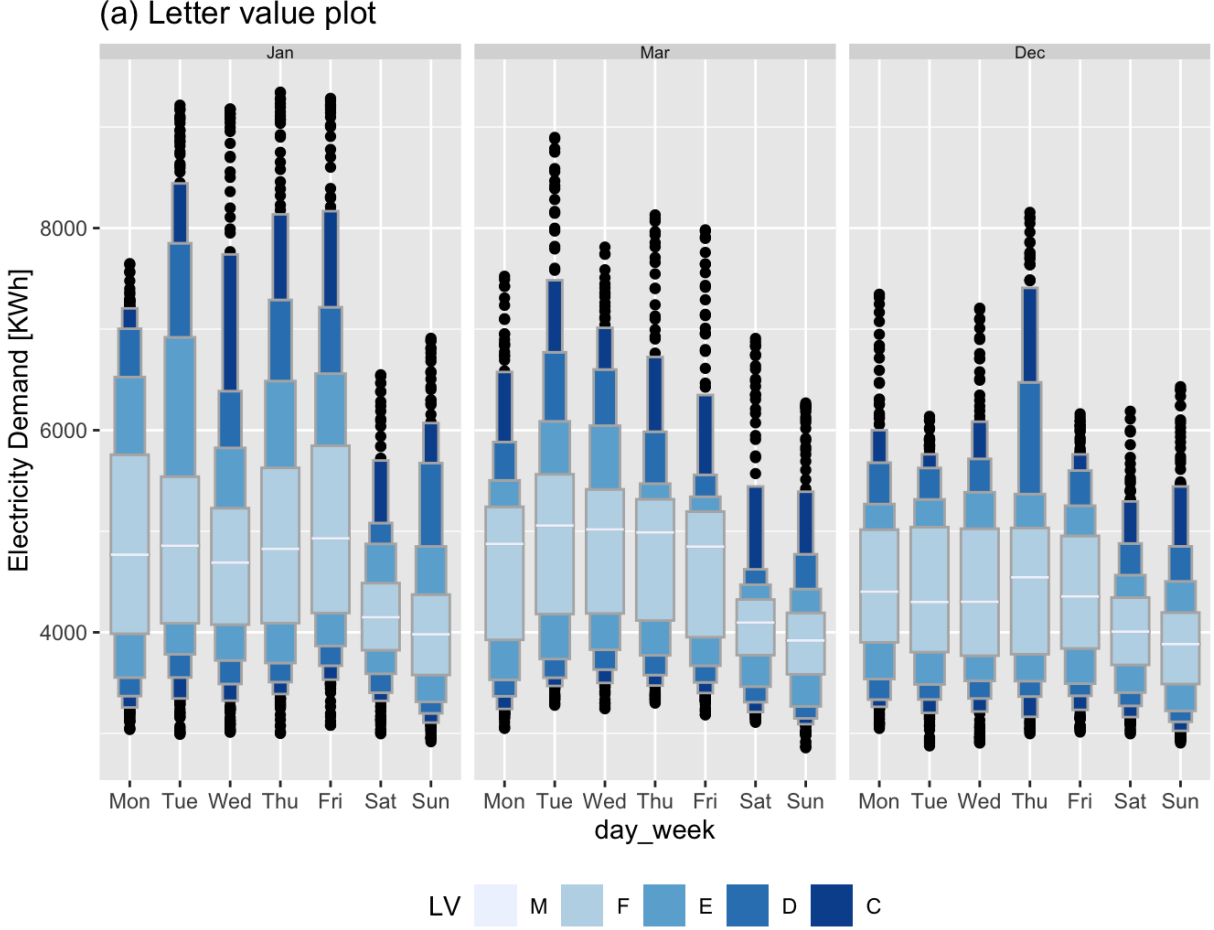
Figure 5: Distribution of energy consumption displayed through letter value plots. Plot (a) displays consumption across month-of-year faceted by quarters of the year, (b) across weekday/weekend faceted by quarters of the year and (c) across quarters of the year faceted by weekday/weekend. Plots (b) and (c) both show harmonies since each quarter consists of both weekdays and weekends. Conversely, weekend and weekday can occur in every quarter. Analysts should avoid plotting such clashes. Plot (b) helps to compare weekends and weekdays for each quarter. It can be seen that for every quarter weekend and weekday consumption are fairly similar except for the second quarter where the letter values below D and E behave differently, whereas, Plot (c) helps to compare quarters within weekdays and weekends. For example, the quartile spread of consumption shrinks/lowers from first to fourth quarter for weekdays, whereas this pattern is not true for weekends. Plot (a) shows a clash since all quarters do not correspond to all months of the year.

5.3 Choosing harmonies to show

The data structure suggests that we look at pairs of cyclic granularities at a time from N_C cyclic granularities. Hence, all possible pairs of cyclic time granularities that could be analyzed together is $^{N_C}P_2$, with each of the circular granularity either mapped to facets or x-axis. Now, if N_C is fairly large, even after excluding clashes, the list of harmonies left would be very large and overwhelming for human consumption. Hence, there is a need to rank the harmonies basis how well they capture the variation in the measured variable and additionally reduce the number of harmonies for further exploration/visualization. Displays that capture more variation within different categories in the same group would be important to bring out different patterns of the data. Hence, the idea would be to select only those harmonies which have significant variation in the measured variable and to rank the selected harmonies, such that a harmony pair is rated more important if the variation between different levels of the x-axis variable is higher on an average across all levels of facet variables. This twofold objective is achieved by defining a statistic that could essentially capture the variation of the measured variable in a harmony pair and constructing a test to check if the variation is statistically significant.

One of the potential ways to evaluate this variation is by computing the maximum pairwise distances between the distributions of the measured variable. A common way to measure distances between distributions is through Jenson-Shanon divergence (Lin (1991)) which is based on Kullback-Leibler divergence (Kullback & Leibler (1951)). The Jensen-Shanon distance between two probability distribution p_1 and p_2 is given by

$$d = [D(p_1, r) + D(p_2, r)]/2 \quad where \quad r = (p_1 + p_2)/2$$

where,

$$D(p_1, p_2) = \int_{-\infty}^{\infty} p_1(x) log \frac{p_1(x)}{p_2(x)} \, dx$$

is the Kullback-Leibler divergence between p_1 and p_2. Probability distributions are estimated through quantiles instead of kernel density so that there is minimal dependency on selecting kernel or bandwidth.

The choice of mapping considered for visualizing data sets $<C_i, C_j, v>$ leads to placing A_k's in close proximity with B_l's representing a group/facet. A harmony pair (C_i, C_j) would be a

more interesting display if the maximum pairwise distance between A_k's $\forall k \in \{1, 2, \ldots, K\}$ are higher for each group/facet. However, these maximum pairwise distances need to be normalized so that the effect of different levels of C_i and C_j are eliminated. Suppose $d_1, d_2 \ldots, d_m$ be a sequence of independent and identically-distributed pairwise distances and $M_m = \max\{d_1, \ldots, d_m\}$. Then Fisher–Tippett–Gnedenko theorem (de Haan & Ferreira 2007) suggests that if a sequence of pairs of real numbers (a_m, b_m) exists such that each $a_m > 0$ and $\lim_{m \to \infty} P\left(\frac{M_m - b_m}{a_m} \leq x\right) = F(x)$, where F is a non-degenerate distribution function, then the limit distribution F belongs to either the Gumbel, Fréchet or Weibull family. The normalizing constants (a_m, b_m) vary depending on the underlying distribution of the pairwise distances. Hence to normalize appropriately, it is important to assume a distribution of these distances.

Menéndez et al. (1997) and Grosse et al. (2002) provide studies of the statistical properties of the Jensen-Shannon divergences and suggest that the theoretical asymptotic distribution of Jensen-Shannon divergence converges to a chi-squared distribution with degrees of freedom equal to the number of discretization used to estimate the continuous distribution. With large degrees of freedom, chi-squared is asymptotically normal by the Central Limit Theorem. Hence, the norming constants for the distribution of M_m are chosen to be $b_m = \Phi^{-1}(1 - 1/m)$ and $a_m = 1/m\phi(b_m)$, where Φ^{-1} and ϕ are the quantile and density function of the limiting normal distribution. Typically normal distributions will have Gumbel limiting distribution for the maxima, which have medians that grow at the rate of $\log m$ as $m \to \infty$. This fact is used to normalize the statistic for different facet levels. The algorithm employed for computing MMPD is summarized as follows:

- **Input:** Data corresponding to all harmony pairs, i.e., data sets of the form (C_i, C_j, v) $\forall i, j \in N_C$

- **Output:** MMPD (Median Maximum Pairwise Distances) measuring the average variation across different levels of C_i and C_j $\forall i, j \in N_C$

1. Fix harmony pair (C_i, C_j).

2. Fix k. Then there are L groups corresponding to level A_k of C_i.

3. Compute $m = \binom{L}{2}$ pairwise distances between distributions of L unordered levels and $m = L - 1$ pairwise distances for L ordered categories.

4. Identify maximum within the m computed distances.

5. Compute normalized maximum distance (NM) using appropriate norming constants.

6. Use Steps 1-5 to compute normalized maximum distance for $\forall k \in \{1, 2, \ldots, K\}$.

7. Compute MMPD $=$ median $(NM_1, NM_2, \ldots, NM_K)/\log(K)$.

8. Repeat Steps 1 to 7 for all harmony pairs.

The algorithm employed for selecting harmonies with significant variation is summarized as follows:

- **Input:** Harmony pairs (C_i, C_j) $\forall i, j \in N_C$

- **Output:** Harmony pairs (C_i, C_j) for which MMPD is significant.

1. Given the measured variable; $\{v_t : t = 0, 1, 2, \ldots, T-1\}$, MMPD is computed for all harmony pairs and is represented by $MMPD_{obs}$.

2. From the original sequence a random permutation is obtained: $\{v_t^* : t = 0, 1, 2, \ldots, T-1\}$.

3. MMPD is computed for all harmony pairs for this random permutation of the data and is represented by $MMPD_{sample}$.

4. Steps (2) and (3) are repeated a large number of times M (e.g. 100).

5. For each permutation, one $MMPD_{sample}$ vector is obtained.

6. 95th percentile of this $MMPD_{sample}$ distribution is computed and stored in $MMPD_{threshold}$.

7. Harmony pairs for which $MMPD_{obs} > MMPD_{threshold}$ are accepted.

5.4 Number of observations and statistical transformations

Visualizing distributions can be misleading if statistical transformations are performed on rarely occurring categories (Section 4.2) or unevenly distributed events. For Kernel density based plots $nobs > 30$ is suggested, for summary statistics based plots like boxplots $nobs = 10$ is acceptable and for quantile plots $nobs$ should at least be equal to the number of quantiles plotted.

Even when there are no rarely occurring events, number of observations might vary hugely within or across each facet. This might happen due to missing observations in the data or uneven locations of events in time domain. In such cases, the statistical transformations based on density should be used with caution as sample sizes would directly affect both the variance and consequently the confidence interval of the estimators.

6 Applications

6.1 Smart meter data of Australia

Smart meters provide large quantities of measurements on energy usage for households across Australia. One of the customer trials (Department of the Environment and Energy 2018) conducted as part of the Smart Grid Smart City project in Newcastle, New South Wales and some parts of Sydney provides customer wise data on energy consumption for every half hour from February 2012 to March 2014. The idea here is to show how to visualize the distribution of the energy consumption across different cyclic granularities in a systematic way to identify different behavioral patterns.

6.1.1 Cyclic granularities search and computation:

The tsibble object `smart_meter10` from R package `gravitas` (Gupta et al. 2019) consisting of `reading_datetime`, `customer_id` and `general_supply_kwh` denoting the index, key and measured variable of the tsibble is used to facilitate the systematic exploration. While trying to explore the energy behavior of these customers systematically across cyclic time granularities, the first thing to consider is which cyclic time granularities we can look at

exhaustively. Let us consider conventional time deconstructions for a Gregorian calendar (second, minute, half-hour, hour, day, week, month, year). Since the interval of this tsibble is 30 minutes, the temporal granularities may range from half-hour to year. Considering 6 linear granularities half-hour, hour, day, week, month and year in the hierarchy table, $N_C = (6 * 5/2) = 15$. If N_C seem too large, the smallest and largest linear granularities could be considered to be removed from the hierarchy table. We remove half-year and year to have $N_C = (4*3/2) = 6$ and obtain cyclic granularities namely "hour_day", "hour_week", "hour_month", "day_week", "day_month" and "week_month", read as "hour of the day", etc. Further, we add cyclic granularity day-type("wknd_wday") to capture weekend and weekday behavior. Now that we have a list of cyclic granularities to look at, we should be able to compute the multiple-order-up granularities using Section 3.4.

6.1.2 Screening and visualizing harmonies

From the search list, $N_C = 7$ cyclic granularities are chosen for which we would like to derive insights of energy behavior. Recalling the data structure $<C_i$, C_j, `general_supply_kwh`$>$ for exploration $\forall i, j \in \{1, 2, \ldots, 7\}$, each of these 7 cyclic granularities can either be mapped to x-axis or to facet. Choosing 2 of the possible 7 granularities, which is equivalent to having $^7P_2 = 42$ candidates for visualization. Fortunately, harmonies can be identified among those 42 possibilities to narrow the search. Table 5 shows 16 harmony pairs after removing clashes and any cyclic granularities with levels more than 31, as effective exploration becomes difficult with many levels (Section 5.2.1). The MMPD is also shown along with indicator (*) only when variation of measured variable across the harmony pair significant. Starting from 42 possible pairs of cyclic granularities to visualize, we are finally left with only 6, which is a very sizable number of displays for exploration.

Few harmony pairs are displayed in Figure 6 to illustrate the siginificance of MMPD, threshold and the impact of different distribution plots and reverse mapping. For each of Figure 6 (b) and (c), C_i is the circular granularity day-type (weekday/weekend) and C_j is hour of the day. The geometry used for displaying the distribution is chosen as area-quantiles and violins in Figure 6 (b and c respectively). Figure 6 (a) displays reverse mapping of C_i and C_j with C_i denoting hour of the day and C_j denoting day-type with

distribution geometrically displayed as boxplots.

In Figure 6 (b), the black line is the median, whereas the purple band covers 25th to 75th percentile, the orange band covers 10th to 90th percentile and the green band covers 1st to 99th percentile. The first facet represents the weekday behavior while the second one displays the weekend behavior and energy consumption across each hours of the day is shown inside each facet. The energy consumption is extremely (positive- or right-) skewed with the 1st, 10th and 25th percentile lying relatively close whereas 75th, 90th and 99th lying further away from each other. This is common across both weekdays and weekends. For the first few hours on weekdays, median energy consumption starts and continues to be higher for longer as compared to weekends.

Consider looking at violin plots instead of quantile plots to look at the same data in Figure 6(c). There is additional information that we can derive looking at the distribution. There is bimodality in the early hours of the day, implying both low and high energy consumption is probable in the early hours of the day both for weekdays and weekends. If we visualize the same data with reverse mapping of the cyclic granularities, then the natural tendency would be to compare weekend and weekday behavior within each hour and not across hours. For example in Figure 6(a), it can be seen that median energy consumption for the early morning hours is extremely high for weekdays compared to weekends. Also, outliers are more prominent in the latter part of the day. All of these indicate that looking at different distribution geometry or changing the mapping might shed lights on different aspect of the energy behavior for the same sample population.

If the data for all keys are visualized together, it might lead to Simpson's paradox, which occurs when one observation shows a particular behavior, but this behavior paradoxically becomes obscured by aggregation. For example in a particular neighborhood one household may have the least daily power consumption for a full week, yet still not be the household with the minimum weekly power consumption. This is an intuitive possibility, because heterogeneous `customer_id`'s with very different occupation or demographics will tend to have very different energy behavior and combining them together will somehow weaken any typical or extreme behavior. A strategy for analyzing multiple keys together could be to first group them basis time series or demographic features and then look at their energy

Table 5: Harmonies with a pair of cyclic granularity one placed on facet and the other on x-axis. Out of 42 possible combinations of cyclic granularities, only 16 are harmony pairs. The harmony pairs are ranked basis highest to lowest MMPD and only the first 6 show significant variation in the measured variable.

facet variable	x-axis variable	facet levels	x-axis levels	MMPD
day_week	day_month	7	31	0.06398*
wknd_wday	day_month	2	31	0.05988*
wknd_wday	hour_day	2	24	0.04361*
day_week	hour_day	7	24	0.02362*
week_month	hour_day	5	24	0.02316*
hour_day	day_month	24	31	0.01592*
day_month	wknd_wday	31	2	0.01359
day_month	day_week	31	7	0.01142
day_month	hour_day	31	24	0.00921
hour_day	wknd_wday	24	2	0.00879
week_month	wknd_wday	5	2	0.00684
day_week	week_month	7	5	0.00429
wknd_wday	week_month	2	5	0.00337
hour_day	week_month	24	5	0.00334
week_month	day_week	5	7	0.0012
hour_day	day_week	24	7	0.00117
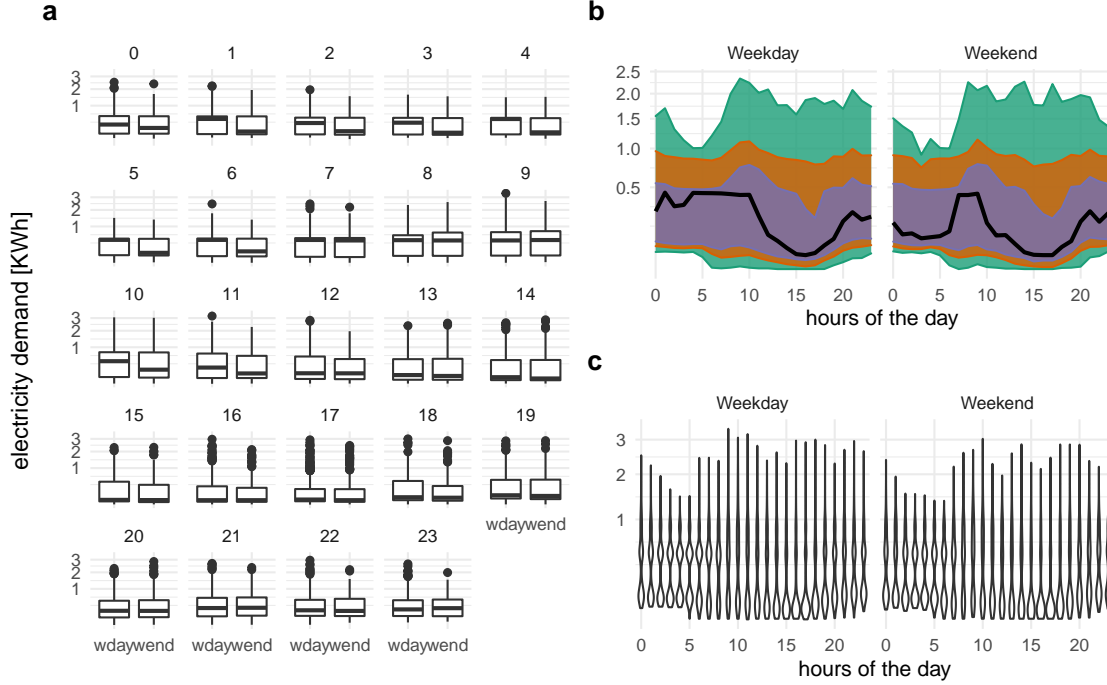
Figure 6: Energy consumption of a single customer shown with different distribution displays, and granularity arrangements. Two granularities are used: hour of the day (I) and weekday/weekend (II). Plot (a) shows granularity I facetted by granularity II, and plots (b), (c) shows the converse mapping. Plot (a) makes a comparison of usage by workday within each hour of the day using side-by-side boxplots. Generally, on a work day there is more consumption early in the day. Plots (b) and (c) examine the temporal trend of consumption over the course of a day, separately for the type of day. Plot (b) uses an area quantile to put the emphasis on the time series, for example, the median consumption over time shows prolonged usage in the morning on weekdays. Plot (c) uses a violin plot to place emphasis on distributional differences across hours. It can be seen that the morning use on weekdays is bimodal, some work days there is low usage, which might indicate the person is working from home and also having a late start.

behavior. This is beyond the scope of the current work.

This case study shows systematic exploration of energy behavior for a household to gain exhaustive insights on periodic behavior of the households.

6.2 T20 cricket data of Indian Premiere League

The method is not only restricted to temporal data, and can be generalized to many hierarchical granularities (with continuous and uni-directional nature). We illustrate this with an application to the sport cricket. Although there is no conventional time component in cricket, each ball can be thought to represent an ordering from past to future with the game progressing forward with each ball. In the Twenty20 format, an over will consist of 6 balls (with some exceptions), an inning is restricted to a maximum of 20 overs, a match will consist of 2 innings and a season consists of several matches. Thus, similar to time, there is a hierarchy where ball is nested within overs, overs nested within innings and innings within matches. The idea of cyclic granularities can be likewise mapped to this hierarchy. Example granularites then include ball of the over, over of the inning and ball of the inning. Although most of these cyclic granularities are circular in design of the hierarchy, in application of the rules some granularities are aperiodic. For example, in most cases an over will consist of 6 balls with some exceptions like wide balls or when an inning finishes before the over finishes. Thus, the cyclic granularity ball-of-over will be circular in most cases and aperiodic in others.

The Indian Premier League (IPL) is a professional Twenty20 cricket league in India contested by eight teams representing eight different cities in India. The ball by ball data for IPL season 2008 to 2016 is fetched from Kaggle. The `cricket` data set in the `gravitas` package summarizes the ball-by-ball data across overs and contains information for a sample of 214 matches spanning 9 seasons (2008 to 2016) such that each over has 6 balls, each inning has 20 overs and each match has 2 innings. This could be useful in a periodic world when we wish to compute any circular/quasi-circular granularity based on a hierarchy table which look like Table 6.

However, even if the situation is not periodic and a similar hierarchy can not be formed, it can be interesting to visualize the distribution of a measured variable across relevant

Table 6: Hierarchy table for cricket where overs are nested within an inning, innings nested within a match and matches within a season.

linear (G)	single-order-up cyclic (C)	period length/conversion operator (K)
over	over-of-inning	20
inning	inning-of-match	2
match	match-of-season	k(match, season)
season	1	1

cyclic granularities to shed light on the aperiodic behavior of a non-temporal data set similar to aperiodic events like formal meetings, workshops, conferences, school semesters in a temporal set up. There are many interesting questions that could possibly be answered with such a data set irrespective of the type of cyclic granularities.

First, it would be interesting to see if the distribution of total runs vary depending on if a team bats in the first or second innings. The Mumbai Indians (MI) and Chennai Super kings (CSK) appeared in final playoffs from 2010 to 2015. We take their example in order to dive deeper into this question. From Figure 7(a), it can be observed that for the team batting in the first inning there is an upward trend of runs per over, while there is no clear upward trend in median and quartile deviation of runs for the teams batting in the second inning. This seem to indicate that players feel mounting pressure to score more runs as they approach towards the end of the first inning. Whereas teams batting in the second inning have a set target in mind and are not subjected to such mounting pressure and may adopt a more conservative strategy, to score runs. Thus winning teams like CSK and MI seem to employ different inning strategies when it comes to their batting order.

Another interesting question could be: do runs per over decrease in the subsequent over if fielding (defending) was good in the previous over? For establishing the fielding quality, we apply an indicator function on dismissals (1 if there was at least one wicket in the previous over due to run out or catch, 0 otherwise). Runs in the current over is then the observation variable. Dismissals in the previous over can lead to a batsman adopting a more defensive play style. Figure 7(b) shows that no dismissals in the previous over leads

to a higher median and quartile spread of runs per over as compared to the case when there has been at least one dismissal in the previous over.

Wickets per over are considered as an aperiodic cyclic granularity with wickets as an aperiodic linear granularity. These granularities do not appear in the hierarchy table since it is difficult to position them in a hierarchy. These are similar to holidays or special events in temporal data.

7 Discussion

Exploratory data analysis and data analysis in general involve many iterations of finding and summarizing patterns. With temporal data available at ever finer scales, exploring periodicity can become overwhelming with so many possible granularities to explore. This work provides a framework to systematically explore distribution of an univariate measured variable across two cyclic time granularities by creating any cyclic granularity, ranking a list of harmonies and thereby identifying possible distribution plots for effective visualization based on relationship and levels of the cyclic granularities.

A missing piece is to enable user-defined temporal calendars. Also, computation of cyclic aperiodic granularities would require computing aperiodic linear granularities first. A few R packages like `almanac` and `gs` provide functionality to create recurring events that are not periodic. These functions can be imported in the `gravitas` package to accommodate for aperiodic cyclic granularities.
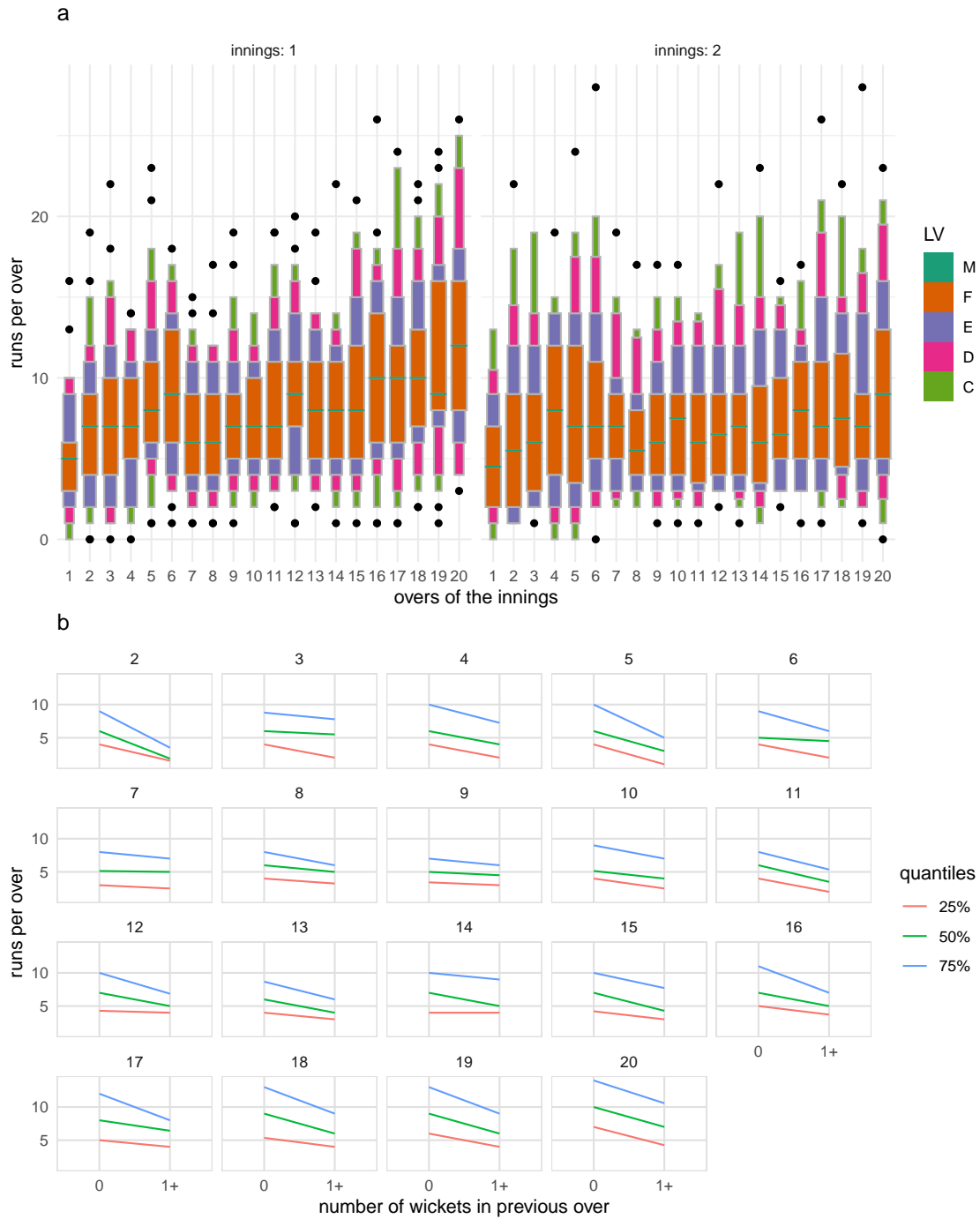
Acknowledgements

Figure 7: Runs per over shown with different distribution displays, and granularities. Plot (a) shows letter value plot across overs faceted by innings. For the team batting in the first innings there is an upward trend of runs per over, while there is no such pattern of runs for the teams batting in the second innings. Plot (b) shows quantile plot of runs per over across an indicator of wickets in previous over faceted by current over. This indicates that at least one wicket in the previous over leads to lower median run rate and quartile spread in the subsequent over.

and `rmarkdown` (Xie et al. 2018, Allaire et al. (2020)). This paper's Github repository, github.com/Sayani07/paper-gravitas, contains all materials required to reproduce this article and the code is also available online in the supplemental materials.

8   Supplemental Materials

Data and scripts: Data sets and R code to reproduce all figures in this article (main.Rmd).

R-package: The ideas presented in this article have been implemented in the open-source R (R Core Team 2019) package `gravitas` (Gupta et al. 2019), available from CRAN. The R-package facilitates manipulation of single and multiple-order-up time granularities through cyclic calendar algebra, check feasibility of creating plots or drawing inferences for any two cyclic granularities by providing list of harmonies and recommend prospective probability distributions through factors described in the article. Version 0.1.2 of the package was used for the results presented in the article and is available on Github (`https://github.com/Sayani07/gravitas`).

R-packages: Each of the R packages used in this article are available online with URLs provided in the bibliography.

References

Aigner, W., Miksch, S., Schumann, H. & Tominski, C. (2011), *Visualization of time-oriented data*, Springer Science & Business Media.

Allaire, J., Xie, Y., McPherson, J., Luraschi, J., Ushey, K., Atkins, A., Wickham, H., Cheng, J., Chang, W. & Iannone, R. (2020), *rmarkdown: Dynamic Documents for R.* R package version 2.1.
URL: *https://github.com/rstudio/rmarkdown*

Bettini, C. & De Sibi, R. (2000), 'Symbolic representation of user-defined time granularities', *Ann. Math. Artif. Intell.* **30**(1), 53–92.

Bettini, C., Dyreson, C. E., Evans, W. S., Snodgrass, R. T. & Wang, X. S. (1998), A

glossary of time granularity concepts, *in* O. Etzion, S. Jajodia & S. Sripada, eds, 'Temporal Databases: Research and Practice', Springer Berlin Heidelberg, Berlin, Heidelberg, pp. 406–413.

de Haan, L. & Ferreira, A. (2007), *Extreme Value Theory: An Introduction*, Springer Science & Business Media.

Department of the Environment and Energy (2018), *Smart-Grid Smart-City Customer Trial Data*, Australian Government, Department of the Environment and Energy.
URL: *https://data.gov.au/dataset/4e21dea3-9b87-4610-94c7-15a8a77907ef*

Dyreson, C., Evans, W., Lin, H. & Snodgrass, R. (2000), 'Efficiently supporting temporal granularities', *IEEE Transactions on Knowledge and Data Engineering* **12**(4), 568–587.

Goodwin, S. & Dykes, J. (2012), Visualising variations in household energy consumption, *in* '2012 IEEE Conference on Visual Analytics Science and Technology (VAST)', IEEE.

Grolemund, G. & Wickham, H. (2011), 'Dates and times made easy with lubridate', *Journal of Statistical Software* **40**(3), 1–25.
URL: *http://www.jstatsoft.org/v40/i03/*

Grolemund, G. & Wickham, H. (2017), *R for data science*, O'Reilly Media.

Grosse, I., Bernaola-Galván, P., Carpena, P., Román-Roldán, R., Oliver, J. & Stanley, H. E. (2002), 'Analysis of symbolic sequences using the Jensen-Shannon divergence', *Phys. Rev. E Stat. Nonlin. Soft Matter Phys.* **65**(4 Pt 1), 041905.

Gupta, S., Hyndman, R., Cook, D. & Unwin, A. (2019), *gravitas: Explore Probability Distributions for Bivariate Temporal Granularities*. R package version 0.1.0.
URL: *https://CRAN.R-project.org/package=gravitas*

Hintze, J. L. & Nelson, R. D. (1998), 'Violin plots: A box Plot-Density trace synergism', *Am. Stat.* **52**(2), 181–184.

Hofmann, H., Wickham, H. & Kafadar, K. (2017), 'Letter-Value plots: Boxplots for large data', *J. Comput. Graph. Stat.* **26**(3), 469–477.

Hyndman, R. J. (1996), 'Computing and graphing highest density regions', *Am. Stat.* **50**(2), 120–126.

Kullback, S. & Leibler, R. A. (1951), 'On information and sufficiency', *Ann. Math. Stat.* **22**(1), 79–86.

Lin, J. (1991), 'Divergence measures based on the shannon entropy', *IEEE Trans. Inf. Theory* **37**(1), 145–151.

Mcgill, R., Tukey, J. W. & Larsen, W. A. (1978), 'Variations of box plots', *Am. Stat.* **32**(1), 12–16.

Menéndez, M. L., Pardo, J. A., Pardo, L. & Pardo, M. C. (1997), 'The Jensen-Shannon divergence', *J. Franklin Inst.* **334**(2), 307–318.

Ning, P., Wang, X. S. & Jajodia, S. (2002), 'An algebraic representation of calendars', *Ann. Math. Artif. Intell.* **36**(1), 5–38.

Potter, K., Kniss, J., Riesenfeld, R. & Johnson, C. R. (2010), 'Visualizing summary statistics and uncertainty', *Comput. Graph. Forum* **29**(3), 823–832.

R Core Team (2019), *R: A Language and Environment for Statistical Computing*, R Foundation for Statistical Computing, Vienna, Austria.
URL: *https://www.R-project.org/*

Reingold, E. M. & Dershowitz, N. (2001), *Calendrical Calculations*, millennium edition edn, Cambridge University Press.

Tukey, J. W. (1977), *Exploratory data analysis*, Addison-Wesley, Reading, Mass.

Wang, E., Cook, D. & Hyndman, R. J. (2020*a*), 'Calendar-based graphics for visualizing people's daily schedules', *Journal of Computational and Graphical Statistics* . to appear.

Wang, E., Cook, D. & Hyndman, R. J. (2020*b*), 'A new tidy data structure to support exploration and modeling of temporal data', *Journal of Computational and Graphical Statistics* . to appear.

Wickham, H. (2016), *ggplot2: Elegant Graphics for Data Analysis*, Springer-Verlag New York.
URL: *http://ggplot2.org*

Wilkinson, L. (1999), *The Grammar of Graphics*, Springer, New York.

Xie, Y. (2015), *Dynamic Documents with R and knitr*, 2nd edn, Chapman and Hall/CRC, Boca Raton, Florida.
URL: *https://yihui.name/knitr/*

Xie, Y. (2020), *knitr: A General-Purpose Package for Dynamic Report Generation in R*. R package version 1.28.
URL: *https://yihui.org/knitr/*

Xie, Y., Allaire, J. & Grolemund, G. (2018), *R Markdown: The Definitive Guide*, Chapman and Hall/CRC, Boca Raton, Florida.
URL: *https://bookdown.org/yihui/rmarkdown*